TRIUMF

PROTON ELASTIC SCATTERING FROM LIGHT NUCLEI

AT INTERMEDIATE ENERGIES

W.T.H. van Oers

Department of Physics
University of Manitoba

MESON FACILITY OF:

UNIVERSITY OF ALBERTA
SIMON FRASER UNIVERSITY
UNIVERSITY OF VICTORIA
UNIVERSITY OF BRITISH COLUMBIA

TRI-77-3

TRI-77-3

TRIUMF

PROTON ELASTIC SCATTERING FROM LIGHT NUCLEI AT INTERMEDIATE ENERGIES

W.T.H. van Oers

Department of Physics
University of Manitoba

Based on a talk presented at the 1976 TRIUMF Users
Group Annual Meeting, December 3-4, 1976

Postal address:

TRIUMF
University of British Columbia
Vancouver, B.C.
Canada V6T 1W5

December 1977

Recent years have seen a wealth of information presented on intermediate-energy proton elastic scattering from very light nuclei (^2H, ^3H, ^3He, and ^4He). It must be said that the energy range studied has a lower limit of approximately 400 MeV. The differential cross-section angular distributions can be thought of as divided into three regions: a forward angular region where one expects the multiple scattering model of Glauber[1] to be valid, this region being characterized by a minimum and secondary maximum caused by the interference of single-scattering and double-scattering amplitudes; a region of intermediate angles where one expects a minimum caused by the interference of double- and triple-scattering amplitudes; and finally the region of backward angles which quite generally exhibits peaking at 180° caused by nucleon or multi-nucleon exchange processes, which may include N*'s or Δ's, and pion emission and reabsorption processes in the 3,3 resonance region.

For orientation Fig. 1 shows $d\sigma/dt$ as a function of the four-momentum transfer variable t [$t = -2k^2(1-\cos\theta)$] in the energy range 150 to 1150 MeV. The solid dots represent data obtained at Saclay with the proton synchrotron SATURNE 1 and the SPES I spectrometer.[2] These data are now considered to be final. The open circles are data obtained with the Berkeley 184-inch synchrocyclotron by a UCLA-LBL-University of Texas collaboration.[3] The filled-in square are the results obtained at 600 MeV with the CERN synchrocylotron by a group from Clermont and Lyon.[4] The open squares, which represent the results obtained at Saclay using an incident α-particle beam and a large-momentum spectrometer,[5] span the entire allowed range of t-values. Finally, the filled triangles give the data obtained with the Orsay synchrocyclotron.[6] One should first of all note that the ratio (R) of the values of the cross-sections at the first minimum [at $t \sim -0.25$ $(GeV/c)^2$] and the second maximum is most pronounced at about 700 MeV (if one excludes for the moment the 600 MeV CERN results). This ratio increases again at higher energies as will be shown below. There is perhaps some indication of a change of slope at around $t = -1.0$ $(GeV/c)^2$ where one expects double- and triple-scattering amplitudes to interfere destructively. At the higher energies the figure does not give the complete range of allowed four-momentum transfer.

At extreme forward angles there is a Coulomb-nuclear interference region which changes from destructive interference to constructive interference because of a change in sign of the real part of the nuclear forward scattering amplitude. This effect is more clearly seen in Fig. 2, which shows the p-^{4}He elastic scattering differential cross-section angular distributions measured prior to 1975 (with the exception of the 156 MeV Orsay data).[7-9] The change in sign of α, the ratio of the real part to the imaginary part of the nuclear scattering amplitude at 0°, can only be determined properly from extreme forward-angle scattering data which contain the interference region. Accurate measurements of the total cross-sections provide a check since the imaginary part of the 0° scattering amplitude is directly related to the total cross-section via the optical theorem [$\mathrm{Im}\, f(0°) = (k/4\pi)\sigma_T$]. One expects α to change sign around 400 MeV. Note that the figure shows a difference between the 1 GeV Brookhaven data and the 1.05 GeV Saclay data. After renormalization and a small angular shift (-0.5°) both angular distributions can be made to agree except for the three data points at the position

of the minimum, which I gathered were the last three points measured in the Brookhaven experiment. It was stated above that the ratio of the cross-sections at the first minimum and at the second maximum increases again for incident proton energies well above 1 GeV. This is demonstrated in Fig. 3, which shows preliminary results of an experiment at 24 GeV using the CERN proton synchrotron.[10] The ratio R has become approximately equal to 4.

It is interesting to note that the first minimum becomes more pronounced at energies where spin and isospin effects are probably small. At 24 GeV there are only small differences between the p-p and n-p scattering parameters. If spin effects contribute significantly then one should have some indication from a p-^{4}He polarization contour diagram. Such a contour diagram based on the existing p-^{4}He polarization data[11] is shown in Fig. 4. One observes that the contour lines tend to close towards 700 MeV (where R as discussed above exhibits a relative maximum). Very large polarizations exist in p-^{4}He elastic scattering, in particular in the energy region of 200 to 300 MeV where polarization values of near +1 and -1 are attained in the forward hemisphere. The ongoing TRIUMF experiment will determine if this pattern persists in the backward hemisphere. (Preliminary results indicate that this is indeed the case.) The current experiment using the ZGS at Argonne National Laboratory will determine if the p-^{4}He polarizations become once more pronounced at higher incident proton energies (i.e., at energies around 3 GeV).

The experimental situation regarding p-^{3}He and p-^{3}H elastic scattering is much more sketchy. The existing differential cross-sections, again plotted versus the four-momentum transfer variable t, are shown in Fig. 5. The open circles present 1.04 GeV data obtained at Saclay with the SPES I spectrometer,[12] the solid dots present 600 MeV data obtained at CERN,[4] the open triangles present 582 MeV data obtained at SREL[9] while the filled triangles present 156 MeV data obtained at Orsay.[13] There exists also p-^{3}H data at 156 MeV[13] and at 600 MeV[4] obtained using gaseous tritium targets containing up to 1000 Ci of tritium. One observes again the characteristic minimum and second maximum due to the interference of single-scattering and double-scattering amplitudes. Note also that there is a break in the slope of the distribution near $t = -1.0\ (\mathrm{GeV}/c)^2$.

In the multiple-scattering eikonal model of Glauber[1] the elastic nucleon-nucleus amplitude takes the form:

$$F(q) = \frac{ik}{2\pi} \int d^3r_1 \ldots d^3r_A\, \rho^{(A)}\left(\vec{r}_1, \ldots \vec{r}_A\right) \delta\left(\sum_i \vec{r}_i\right)$$

$$\times \int d^2b\, e^{i\vec{q}\vec{b}} \left[1 - \prod_{j=1}^{A} \left(1 - \frac{1}{2\pi i k_o} \int d^2q\, e^{-i\vec{q}(\vec{b}-\vec{s}_j)}\, f_j(q)\right)\right]. \qquad (1)$$

In this expression f_j represents the two-particle amplitude for the scattering of the projectile from the jth target nucleon; k_o and k are the incident momentum in the nucleon-nucleon and nucleon-nucleus centre-of-mass system, respectively; and $\vec{q}$ is the momentum transfer. The nuclear structure information is contained in the many-body

ground state density $\rho^{(A)}(\vec{r}_1,\ldots,\vec{r}_A)$ of the target nucleus; the vector $\vec{s}_j$ represents the projection of the position $\vec{r}_j$ of the jth nucleon in the plane normal to the incident direction.

One usually assumes that the target nucleon overlap is negligible and consequently the phases are additive, which in turn allows one to introduce the experimentally determined nucleon-nucleon amplitudes $f_j(q)$. But this is an assumption which really is not very good, since the inter-nucleon spacing is of the order of 1 fm (well within the range of the strong interaction, of course), and thus one requires a knowledge of the nucleon-nucleon off-energy-shell interaction. One also assumes that the average Coulomb phase, calculated from the total charge distribution, can simply be added to the strong interaction phases. The Coulomb interaction has a noticeable influence not only at extreme forward angles but also at the diffraction minima where it interferes according to the sign of the real part of f_j.

The most general representation of the nucleon-nucleon scattering amplitude consists of five amplitudes:

$$M(q) = A(q) + C(q)(\vec{\sigma}_o+\vec{\sigma}_j)\cdot\hat{n} + M'(q)(\vec{\sigma}_o\cdot\hat{n})(\vec{\sigma}_j\cdot\hat{n}) + G(q)[(\vec{\sigma}_o\cdot\hat{P})(\vec{\sigma}_j\cdot\hat{P}) + (\vec{\sigma}_o\cdot\hat{k})(\vec{\sigma}_o\cdot\hat{k})] + H(q)[(\vec{\sigma}_o\cdot\hat{P})(\vec{\sigma}_j\cdot\hat{P}) - (\vec{\sigma}_o\cdot\hat{k})(\sigma_j\cdot\hat{k})] \tag{2}$$

using standard notation, see for instance Ref. 14, and $\hat{n}$, $\hat{P}$, and $\hat{k}$ are unit vectors in the direction of $\vec{k}_o \times \vec{k}_F$, $\vec{k}_o + \vec{k}_F$, and $\vec{k}_o - \vec{k}_F$. Of these one usually retains only two amplitudes

$$M(q) \simeq A(q) + C(q)(\vec{\sigma}_o+\vec{\sigma}_j)\cdot\hat{n}. \tag{3}$$

The amplitudes A and C are parametrized in a form suggested by the optical theorem for diffractive scattering and frequently used at high energies

$$A(q) = \frac{\sigma_T\, k_o}{4\pi}(i+\alpha)\exp(-\beta\, q^2/2) \tag{4}$$

for the spin-independent part and

$$C(q) = \frac{\sigma_T\, k_o}{4\pi}\, i\sqrt{\frac{q^2}{4m^2}}\,(i+\alpha_s)D_s\exp(-\beta_s\, q^2/2) \tag{5}$$

for the spin-dependent part. In these expressions σ_T is the total cross-section, $\alpha(\alpha_s)$ the ratio of real to imaginary parts of the amplitude, $\beta(\beta_s)$ the slope parameter, D_s the relative strength of the spin-dependent amplitude, and m is the nucleon mass. Note that in these expressions one assumes that the real part and the imaginary part of the amplitude have the same q dependence.

It is obvious that one would prefer the use of a more complete parameterization of the nucleon-nucleon scattering amplitudes. However, the lack of precise nucleon-nucleon scattering data, especially at forward angles (which is the region of importance for nucleon-nucleus scattering) and in particular at energies above 500 MeV, at present

prevents the deduction of the corresponding scattering amplitudes in a reliable manner. I would like to draw attention to the current uncertainties with regard to α as extracted from forward-angle p-p scattering data at energies up to roughly 1 GeV,[15] not to mention the situation with regard to α for the n-p system. The analysis of the nucleon-nucleon scattering data is furthermore increasingly complicated as a result of the increasing inelasticity. Figure 6 shows α, the ratio of the real part to the imaginary part of the forward p-p non-spin-flip scattering amplitude as deduced in the phase-shift analyses of Bystricky and Lehar (shaded bands).[16] Curve a) represents α as deduced from the energy-dependent phase-shift analysis of MacGregor *et al.*, and curves b) and c) are dispersion relation calculations of Söding and Dumbrais, respectively (see Ref. 15). Figure 7 shows the behaviour of α_{pp} and α_{np} as a function of energy.[17] The values of α_{pp} were obtained by fitting the forward-angle p-p elastic scattering data with an expression of the form

$$\frac{d\sigma}{dt} = 4\pi \frac{(zZ\alpha)^2\hbar^2}{\beta^2|t|^2}\exp(bt) - \frac{zZ\alpha}{\beta|t|}\sigma_T\,(\sin 2\delta + \alpha_{pp}\cos 2\delta)\exp(bt)$$

$$+ \frac{1}{16\pi}\sigma_T^2\left(1 + \alpha_{pp}^2\right)\frac{1}{\hbar^2}\exp(bt), \qquad (6)$$

where α is the fine structure constant, βc is the velocity of the incident particle, $z = Z = 1$, b is the form factor slope parameter, δ is the Bethe phase, $\delta = (-\frac{1}{2}\ln|t| - \ln b + \ln 2 - \gamma)\frac{zZ\alpha}{\beta}$, and γ is Euler's constant.

The nuclear structure enters the problem either through the N-body density $\rho^{(N)}(\vec{r}_1,\ldots\vec{r}_N)$ or the one-body density $\rho(r)$. One usually proceeds through a one-body density,

$$\rho(r) = N\left(e^{-\kappa_1^2 r^2} - C\,e^{-\kappa_2^2 r^2}\right), \qquad (7)$$

and determines the parameters by a fit to the charge form factor.

The results obtained by Auger, Gillespie and Lombard,[18] which include corrections due to target-nucleon overlap and charge exchange, give rather good agreement with the p-^{4}He differential cross-sections but rather poor agreement with the p-^{4}He polarizations. Figures 8 and 9 show the results of their calculations at 1.15 GeV and 24 GeV. It should be remarked that before one can get to the details of the nuclear target wave function many of the approximations made need a great deal more investigation.

Rule and Hahn[19] made an effective channel analysis of p-^{4}He elastic scattering. In their approach the intermediate-energy proton-nucleus scattering is formulated in terms of coupled equations in which the effects of inelastic processes, which are specifically associated with the excitations of the target system during the collision, are represented by an average inelastic channel. The theory incorporates approximately the effects of nonlocality, energy dependence, rescattering and absorption of all the inelastic channels. Fair agreement with the p-^{4}He differential cross-section angular distributions has been obtained. Spin-dependent effects have been ignored.

Phenomenological optical-model analyses of p-^{4}He elastic scattering have most recently been made by Arnold *et al.*[20] The optical potential used has the form

$$U = (V + iW)\, f(r), \tag{8}$$

with the shape function f(r) given by a three-parameter Fermi distribution

$$f(r) = \frac{1 + wr^2/c^2}{1 + \exp[(r-c)/z]}. \tag{9}$$

The potential is inserted in the Dirac equation as the fourth component of a four-vector, with the vector part of the potential taken to be zero. Note that spin-dependent effects are not considered. Very good fits to the forward differential cross-section data are obtained, as shown in Fig. 10. The volume integral per nucleon of the central potential, as defined by

$$J/A = \int \frac{U(r)d^3r}{A}, \tag{10}$$

has the characteristic energy dependence

$$J_R/A = J_o/A + \beta \ln T_p, \tag{11}$$

also found from optical-model analyses of proton elastic scattering at intermediate energies from various nuclei throughout the periodic table.[21] The energy dependence of J/A for p-^{4}He obtained by Arnold *et al.* is shown in Fig. 11. The real part of the potential changes sign at around 400 MeV. This compares very favourably with what obtained from the analyses of proton elastic scattering from heavier nuclei (see Fig. 12). Note the difference in the sign convention. For a nucleus as light as ^{4}He one has to restrict the data to be fitted to the forward angular region where contributions from the exchange amplitude are small.

Considerable attention has been given to the anomalies in the backward hemisphere of the angular distributions of protons elastically scattered from ^{2}H, ^{3}He and ^{4}He. These anomalies are easily recognizable in the 180° excitation functions where they appear as a secondary maximum at ∿500 MeV in the case of ^{2}H(p,p)^{2}H and as pronounced changes in the slopes in the case of ^{3}He(p,p)^{3}He and ^{4}He(p,p)^{4}He. Figure 13 shows the p-d 180° excitation function.[11] The open circles present neutron data while the solid dots represent proton data. A simple neutron exchange mechanism fails to explain the p-d backward angle distributions around the energy of the second maximum even after both $^3S_1$ and $^3D_1$ components of the deuteron wave function have been taken into account. It should be noted that, to first order, the backward angle differential cross-sections are proportional to $|\phi(|\vec{q}|)|^4$ where $|\vec{q}|$ is the magnitude of the momentum transfer. Thus the backward angle differential cross-section is extremely sensitive to the details of the wave function at large momenta. The p-d backward-angle distributions have been explained using various hypotheses, i.e., the exchange of nucleon resonances,[22] and high-order multiple scattering.[23] Gurvitz, Alexander and Rinat[24] have formulated a noneikonal

approach to hadron-nucleus scattering valid for all angles but for incident momenta greater than 1 GeV/c or in the case of proton scattering for incident energies greater than approximately 500 MeV. They obtain agreement with the experimental p-d data over a large part of the differential cross-section angular distributions and also backward peaking, but there is no quantitative agreement. Unfortunately, their theory is not valid in the energy region where the 180° excitation function shows a relative maximum, i.e., around 500 MeV. Thus, no detailed quantitative agreement with the experimental data has been presented as yet, and the possible existence of nucleon resonances in nuclei is still an intriquing problem indeed.

A polarization contour diagram (Fig. 14), based on the existing data of the polarization of protons elastically scattered from deuterium,[25,9] reveals rapid changes towards the energy where the relative maximum in the 180° excitation function occurs. At the resonant energy, due to the large value of the cross-section for the reaction $p + N \rightarrow d + \pi$ the two-step process, shown in the insert in Fig. 15, may become important. In this two-step process the incident proton interacts with one of the nucleons of the deuteron initiating the reaction $p + d \rightarrow d + \pi$. The pion is successively reabsorbed by the other nucleon. Using this model predictions of the p-d backward angle polarizations have been made.[26] These predictions are depicted as solid dots in the figure. Preliminary values for the p-d polarization at 630 MeV, obtained at Dubna,[26] are shown as open circles. The curve is drawn only to guide the eye. The asymmetry angular distribution at 630 MeV would indicate even more pronounced changes than shown in the polarization contour diagram (Fig. 15). It should be noted that the same model fails to give any resemblance with the experimental polarization angular distribution at 425 MeV.

The p-^{4}He backward angular distributions plotted as function of $\cos\theta$ are shown in Fig. 16. Note that the angular distributions for increasing energy first show an increase towards 180°, then a slowly decreasing or flat behaviour followed by another increase towards 180° at the two highest energies. The data at 298, 438, 648, and 840 MeV were obtained at Saclay using an α-particle beam incident on a hydrogen target and the large-momentum spectrometer.[5] The horizontal error bars present the angular acceptance in the centre-of-mass system. In the laboratory the α-particles are restricted to a forward cone with half-angle of $\sim$14.6°. The resulting 180° excitation function is shown in Fig. 17.[27] Here the anomalous behaviour of the angular distributions corresponds to a change in slope at around 200 MeV. The shoulder at about 40 MeV is caused by a particular interplay of the p-wave and d-wave p-^{4}He phase shifts. Lesniak, Lesniak and Tekou[28] have calculated backward p-^{4}He angular distributions in the framework of a triton exchange model including absorption in the initial and final states. They found that absorption can diminish the cross-sections obtained in the Born approximation by one or two orders of magnitude. The calculated angular distributions give fair agreement with the experimental data at 298, 438, and 648 MeV, as shown in Fig. 18. These authors predict additional structure in the angular distributions around 240 MeV, with possibly a minimum in the excitation function.

The p-^{4}He backward angular distributions plotted as function of $\cos\theta$ are shown in Fig. 19.[29,7,13] Note that all measured angular distributions show peaking towards 180°

but the decrease in the value of the differential cross-sections is non-monotonic. The data at 415, 600, and 800 MeV were obtained at Saclay with the SPES I spectrometer. The 180° excitation function shows a shoulder around 400 MeV (Fig. 20). The curve is drawn to guide the eye and has no further significance. In summary, it is apparent that the backward angle anomalies in p-d, p-^{3}He and p-^{4}He elastic scattering require a great deal further experimental and theoretical attention, including measurements of the asymmetries using an incident polarized proton beam, before a quantitative description of the underlying physical process can be given.

References

1. R.J. Glauber, in *Lectures in Theoretical Physics*, ed. by W.E. Brittin and L.G. Dunham (Interscience, New York, 1959), vol 1, p.315.
2. E. Aslanides, T. Bauer, R. Bertini, R. Beurtey, A. Boudard, F. Brochard, G. Bruge, A. Chaumeaux, H. Catz, J.M. Fontaine, R. Frascaria, D. Garreta, P. Gorodetzky, J. Guyot, F. Hibou, M. Matoba, Y. Terrien, and J. Thirion, contribution IV.A.14 to VI Int. Conf. on High-Energy Physics and Nuclear Structure, Santa Fe and Los Alamos, 1975; D. Legrand, private communication.
3. S.L. Verbeck, J.C. Fong, G.J. Igo, C.A. Whitten, Jr., D.L. Hendrie, Y. Terrien, V. Perez-Mendez, and G.W. Hoffmann, Phys. Lett. 59B, 339 (1975).
4. J. Fain, J. Gardes, A. Lefort, L. Meritet, J.F. Pauty, G. Peynet, M. Querrou, F. Vazeille, and B. Ille, Nucl. Phys. A262, 413 (1976).
5. J. Berger, J. Duflo, L. Goldzahl, F. Plouin, J. Oostens, M. van den Bossche, L. Vu-Hai, G. Bizard, C. Le Brun, F.L. Fabbri, P. Picozza, and L. Satta, Phys. Lett. 63B, 111 (1976); Phys. Rev. Lett. 37, 1195 (1976).
6. V. Comparat, R. Frascaria, N. Fujiwara, N. Marty, M. Morlet, P.G. Roos, and A. Willis, Phys. Rev. C 12, 251 (1975).
7. L.G. Votta, P.G. Roos, N.S. Chant, and R. Woody,III, Phys. Rev. C 10, 520 (1974).
8. N.P. Goldstein, A. Held, and D.G. Stairs, Can. J. Phys. 48, 2629 (1970); A.M. Cormack, J.N. Palmieri, N.F. Ramsey, and R. Wilson, Phys. Rev. 115, 599 (1959); K. Gotow, University of Rochester report NYO-2532, unpublished; O. Chamberlain, E. Segrè, R.D. Tripp, C. Wiegand, and T. Ypsilantis, Phys. Rev. 102, 1659 (1956); V.I. Komarov, G.E. Kosarev, and O.V. Savchenko, Sov. J. Nucl. Phys. 11, 399 (1970); H. Palevsky, J.L. Friedes, R.J. Sutter, G.W. Bennett, G.J. Igo, W.D. Simpson, G.C. Phillips, D.M. Corley, N.S. Wall, R.L. Stearns, and B. Gottschalk, Phys. Rev. Lett. 18, 1200 (1967); S.D. Baker, R. Beurtey, G. Bruge, A. Chaumeaux, J.M. Durand, J.C. Faivre, J.M. Fontaine, D. Garreta, D. Legrand, J. Saudinos, J. Thirion, R. Bertini, F. Brochard, and F. Hibou, Phys. Rev. Lett. 32, 839 (1974).
9. E.T. Boschitz, W.K. Roberts, J.S. Vincent, M. Blecher, K. Gotow, P.C. Gugelot, C.F. Perdrisat, L.W. Swenson, and J.R. Priest, Phys. Rev. C 6, 457 (1972).
10. J. Berthot, G. Douhet, J. Gardès, L. Méritet, M. Querrou, A. Têtefort, F. Vazeille, J.P. Burq, M. Chemarin, M. Chevallier, B. Ille, M. Lambert, J.P. Marin, J.P. Gerber, and C. Voltini, contribution VI.A.8 to VI Int. Conf. on High-Energy Physics and Nuclear Structure, Santa Fe and Los Alamos, 1975.
11. W.T.H. van Oers, in *Few Body Problems in Nuclear and Particle Physics*, ed. by R.J. Slobodrian, B. Cujec, and K. Ramavataram (Les Presses de l'Université Laval, Québec, 1975), p.307.
12. R. Frascaria, N. Marty, V. Comparat, M. Morlet, A. Willis, D. Legrand, D. Garreta, R. Beurtey, G. Bruge, P. Couvert, H. Catz, A. Chaumeaux, J.C. Faivre, Y. Terrien, and R. Bertini, contribution IV.A.12 to VI Int. Conf. on High-Energy Physics and Nuclear Structure, Santa Fe and Los Alamos, 1975.
13. H. Langevin-Joliot, Ph. Narboni, J.P. Didelez, G. Duhamel, L. Marcus, and M. Roy-Stephan, Nucl. Phys. A158, 309 (1970).
14. B.P. Nigam, Rev. Mod. Phys. 35, 117 (1963).

15. D. Aebischer, B. Favier, L.G. Greeniaus, R. Hess, A. Junod, C. Lechanoine, J.C. Niklès, D. Rapin, C. Richard-Serre, and D.W. Werren, Phys. Rev. D 13, 2478 (1976).

16. J. Bystricky and F. Lehar, Proc. Fourth Int. Symp. on Polarization Phenomena in Nuclear Reactions, ed. by W. Gruebler and V. König (Birkhäuser, Basel, 1976), p.458.

17. For α_{pp}:
D. Aebischer *et al.*, Ref. 15; L.M.C. Dutton and H.B. van der Raay, Phys. Lett. 26B, 679 (1968); A.A. Vorobyov *et al.*, Phys. Lett. 41B, 639 (1972); L.F. Kirillova *et al.*, Sov. Phys.—JETP 23, 52 (1966); A.E. Taylor *et al.*, Phys. Lett. 14, 54 (1965); K.J. Foley *et al.*, Phys. Rev. Lett. 19, 857 (1967); G.G. Beznogikh *et al.*, Phys. Lett. 39B, 411 (1972); G. Belletini *et al.*, Phys. Lett. 14, 164 (1965); U. Amaldi *et al.*, Phys. Lett. 43B, 231 (1973); V. Bartenev *et al.*, Phys. Rev. Lett. 31, 1367 (1973).
For α_{np}:
as determined in phase shift analyses: M.H. MacGregor and R.A. Arndt, Phys. Rev. 139, B362 (1965); H.P. Noyes, D.S. Bailey, R.A. Arndt, and M.H. MacGregor, Phys. Rev. 139, B380 (1965); Yu.M. Kazarinov and V.S. Kiselev, Zh. Eksp. Teor. Fiz. 46, 797 (1964) [Sov. Phys.—JETP 19, 542 (1964)]; L.M.C. Dutton and H.B. van der Raay, Phys. Lett. 21, 1416 (1968); N. Dalkhazhav *et al.*, Sov. J. Nucl. Phys. 8, 196 (1969); L.S. Zolin *et al.*, Sov. J. Nucl. Phys. 12, 182 (1971); G.G. Beznogikh *et al.*, Sov. J. Nucl. Phys. 18, 179 (1974); G. Belletini *et al.*, Phys. Lett. 19, 341 (1965); V. Franco and G.K. Varma, Phys. Rev. C 12, 225 (1975).

18. J.P. Auger, J. Gillespie, and R.J. Lombard, Nucl. Phys. A262, 372 (1976).

19. Y. Hahn and D.W. Rule, Phys. Rev. C 12, 1607 (1975); D.W. Rule and Y. Hahn, Phys. Rev. C 12, 1616 (1975); Phys. Rev. Lett. 34, 332 (1975); D.W. Rule and Y. Hahn, Phys. Rev. C 14, 1102 (1976).

20. L.G. Arnold, B.C. Clark, R.L. Mercer, D.G. Ravenhall, and A.M. Saperstein, Phys. Rev. C 14, 1878 (1976); L.G. Arnold, B.C. Clark, and R.L. Mercer, Phys. Rev. C 15, to be published; B.C. Clark, private communication.

21. W.T.H. van Oers and H. Haw, Phys. Lett. 45B, 227 (1973).

22. A.K. Kerman and L.S. Kisslinger, Phys. Rev. 180, 1483 (1969); L.S. Kisslinger, *High-Energy Physics and Nuclear Structure*, ed. by S. Devons (Plenum, New York, 1970), p.816.

23. L. Bertocchi and A. Capella, Nuovo Cimento A51, 369 (1967).

24. S.A. Gurvitz, Y. Alexander, and A.S. Rinat, Ann. Phys. (N.Y.) 94, 223 (1975); *ibid.* 98, 346 (1976).

25. J.C. Faivre, D. Garreta, J. Jungerman, A. Papineau, J. Sura and A. Tarrats, Nucl. Phys. A127, 169 (1969); A.R. Johnston, W.R. Gibson, E.A. McClatchie, J.H.P.C. Megaw, G.T.A. Squier, R.J. Griffiths, and F.G. Kingston, Rutherford Laboratory report RHEL/R-136, unpublished; S.N. Bunker, J.M. Cameron, R.F. Carlson, J.R. Richardson, P. Tomaš, W.T.H. van Oers, and J.W. Verba, Nucl. Phys. A113, 461 (1968); H.E. Conzett, H.S. Goldberg, E. Shield, R.J. Slobodrian, and S. Yamabe, Phys. Lett. 11, 68 (1964); M. Poulet, A. Michalowicz, Y. LeGuen, K. Kuroda, D. Cronenberger, and G. Coignet, J. Physique 26, 399 (1965); H. Postma and R. Wilson, Phys. Rev. 121, 1229 (1961) (these data have been multiplied by a renormalization factor of 0.933, see K. Kuroda *et al.* below); K. Kuroda, A. Michalowicz, and M. Poulet, Nucl. Phys. 88, 33 (1966); N.E. Booth, C. Dolnick, R.J. Esterling, J. Parry, J. Scheid, and D. Sherden, Phys. Rev. D 4, 1261 (1971).

26. L.I. Lapidus, Proc. VI Int. Conf. on High-Energy Physics and Nuclear Structure, ed. by D.E. Nagle, A.S. Goldhaber, C.K. Hargrave, R.L. Burman, and B.G. Storms, AIPCP No. 26 (American Institute of Physics, New York, 1975), p.129.

27. A. Houdayer, private communication.

28. H. Leśniak, L. Leśniak, and A. Tekou, Nucl. Phys. A267, 503 (1976).

29. B.T. Murdoch, private communication; S.A. Harbison, R.J. Griffiths, N.M. Stewart, A.R. Johnston, and G.T.A. Squier, Nucl. Phys. A150, 570 (1970); J.R. Morales, T.A. Cahill, D.J. Shadoan, and H. Willmes, Phys. Rev. C 11, 1905 (1975); L.G. Votta, P.G. Roos, N.S. Chant, and R. Woody, III, Phys. Rev. C 10, 520 (1974); R. Frascaria, I. Brissaud, N. Marty, M. Morlet, F. Reide, A. Willis, R. Beurtey, A. Boudard, M. Garcon, G.A. Moss, Y. Terrien, and W.T.H. van Oers, Phys. Lett. 66B, 329 (1977).

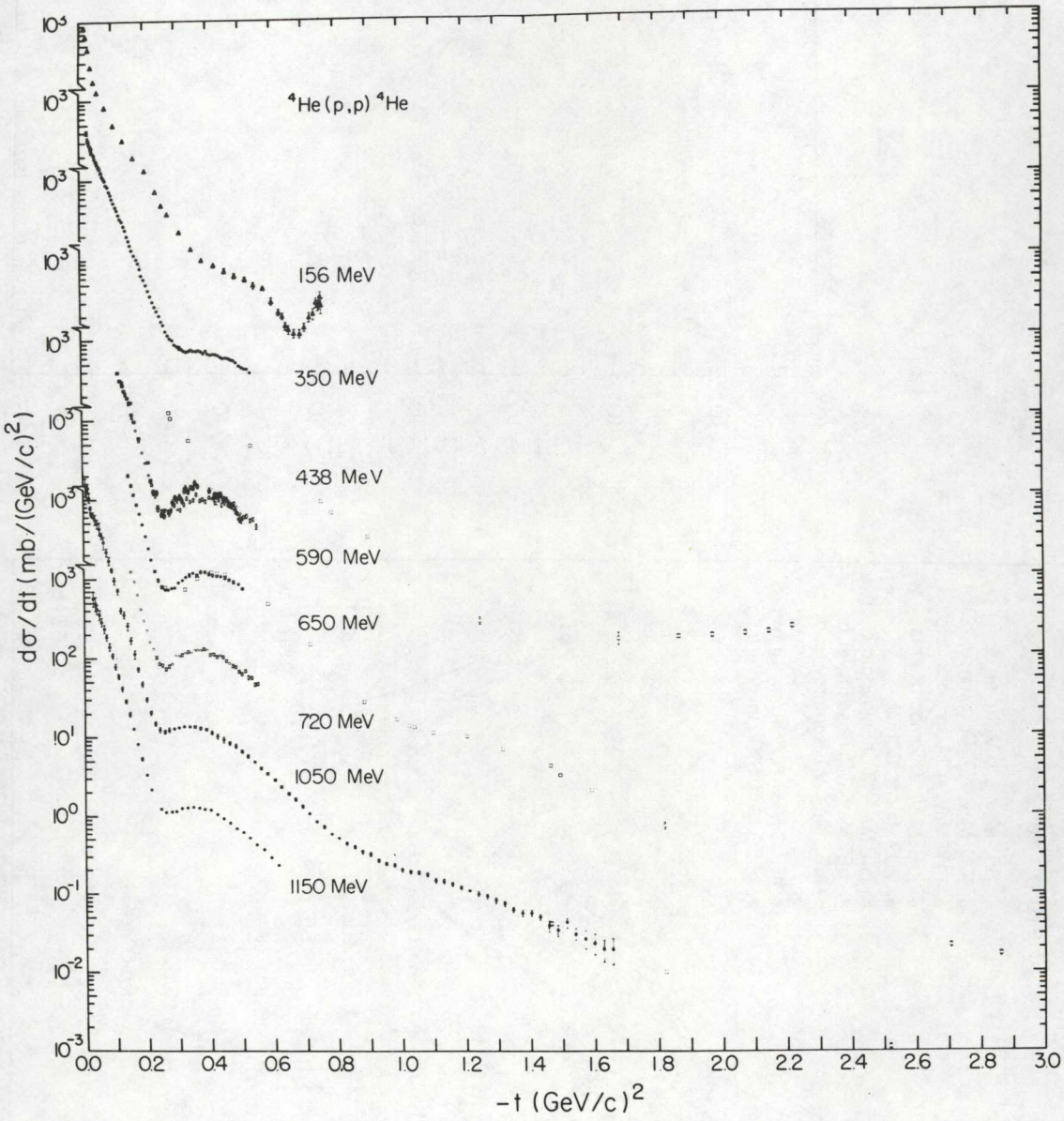
^{4}He(p,p)^{4}He
156 MeV
350 MeV
438 MeV
590 MeV
650 MeV
720 MeV
1050 MeV
1150 MeV
dσ/dt (mb/(GeV/c)^2)
-t (GeV/c)^2

Fig. 1

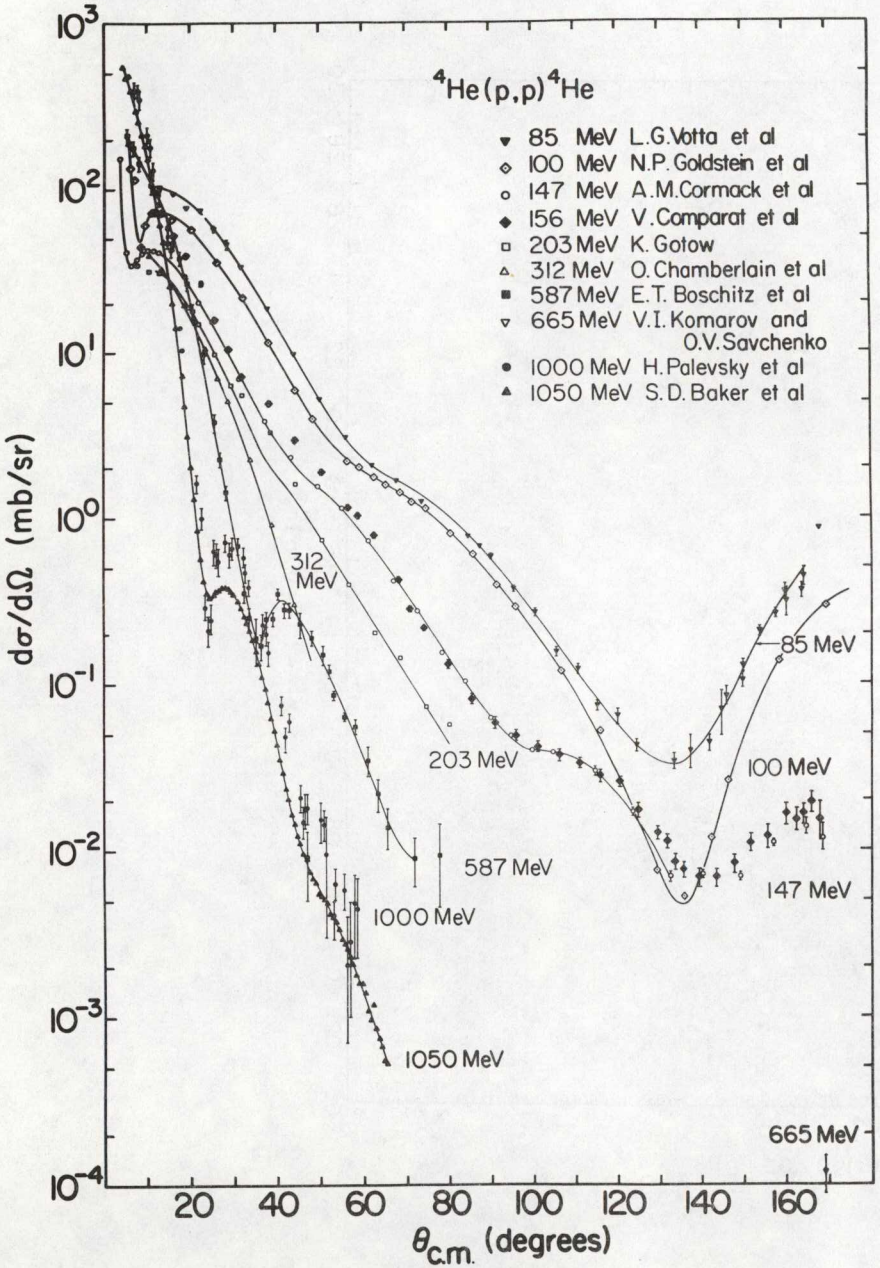
^{4}He(p,p)^{4}He
85 MeV L.G.Votta et al
100 MeV N.P.Goldstein et al
147 MeV A.M.Cormack et al
156 MeV V.Comparat et al
203 MeV K.Gotow
312 MeV O.Chamberlain et al
587 MeV E.T.Boschitz et al
665 MeV V.I.Komarov and O.V.Savchenko
1000 MeV H.Palevsky et al
1050 MeV S.D.Baker et al
312 MeV
203 MeV
587 MeV
1000 MeV
1050 MeV
85 MeV
100 MeV
147 MeV
665 MeV
dσ/dΩ (mb/sr)
θc.m. (degrees)

Fig. 2

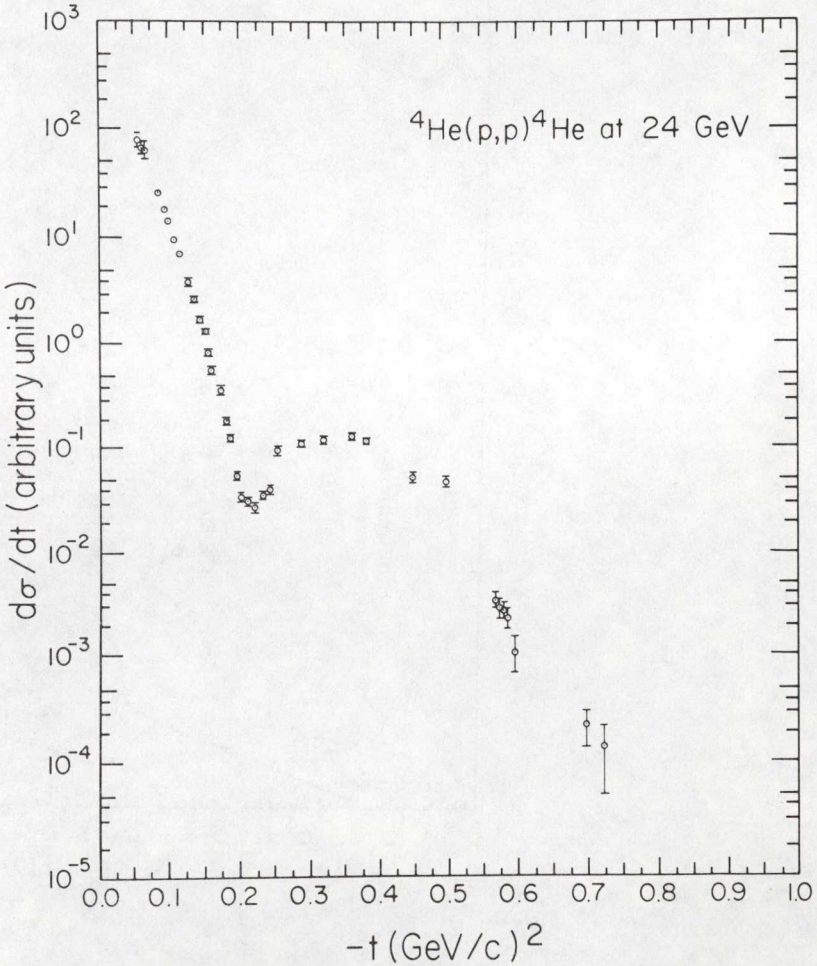
^{4}He(p,p)^{4}He at 24 GeV
dσ/dt (arbitrary units)
-t (GeV/c)^2

Fig. 3

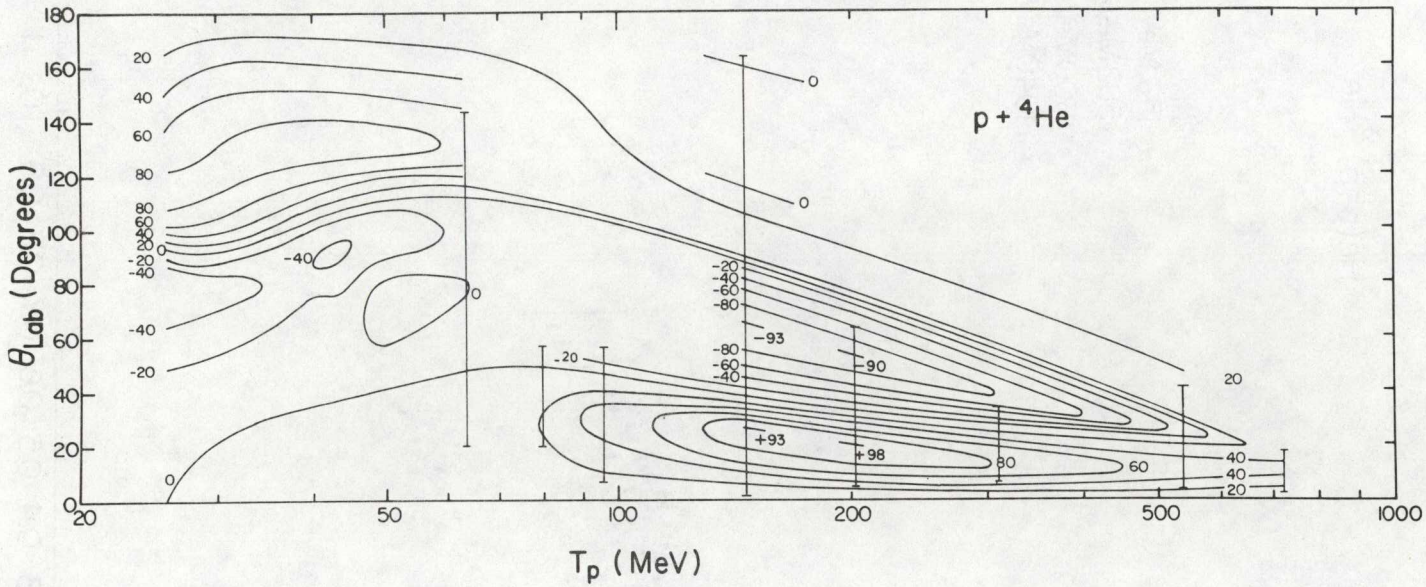
p + 4He
θLab (Degrees)
Tp (MeV)
180
160
140
120
100
80
60
40
20
0
20
50
100
200
500
1000
20
40
60
80
80
60
40
20
0
-20
-40
-40
-20
0
-40
0
-20
0
0
-20
-40
-60
-80
-93
-80
-60
-40
90
+93
+98
80
60
20
40
40
20

Fig. 4

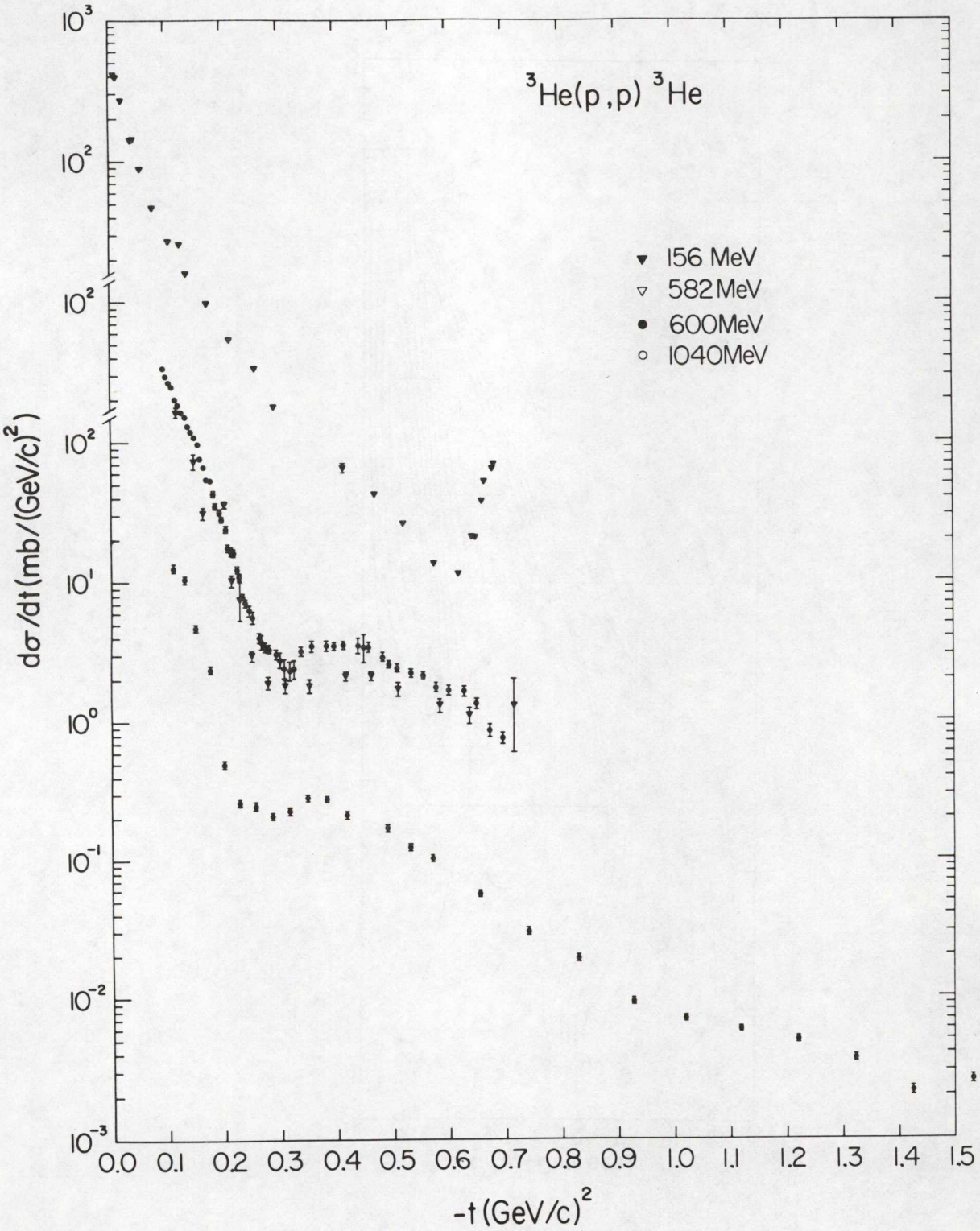
^{3}He(p,p) ^{3}He
156 MeV
582 MeV
600 MeV
1040 MeV
dσ/dt (mb/(GeV/c)^2)
-t (GeV/c)^2
10^3
10^2
10^2
10^2
10^1
10^0
10^{-1}
10^{-2}
10^{-3}
0.0 0.1 0.2 0.3 0.4 0.5 0.6 0.7 0.8 0.9 1.0 1.1 1.2 1.3 1.4 1.5

Fig. 5

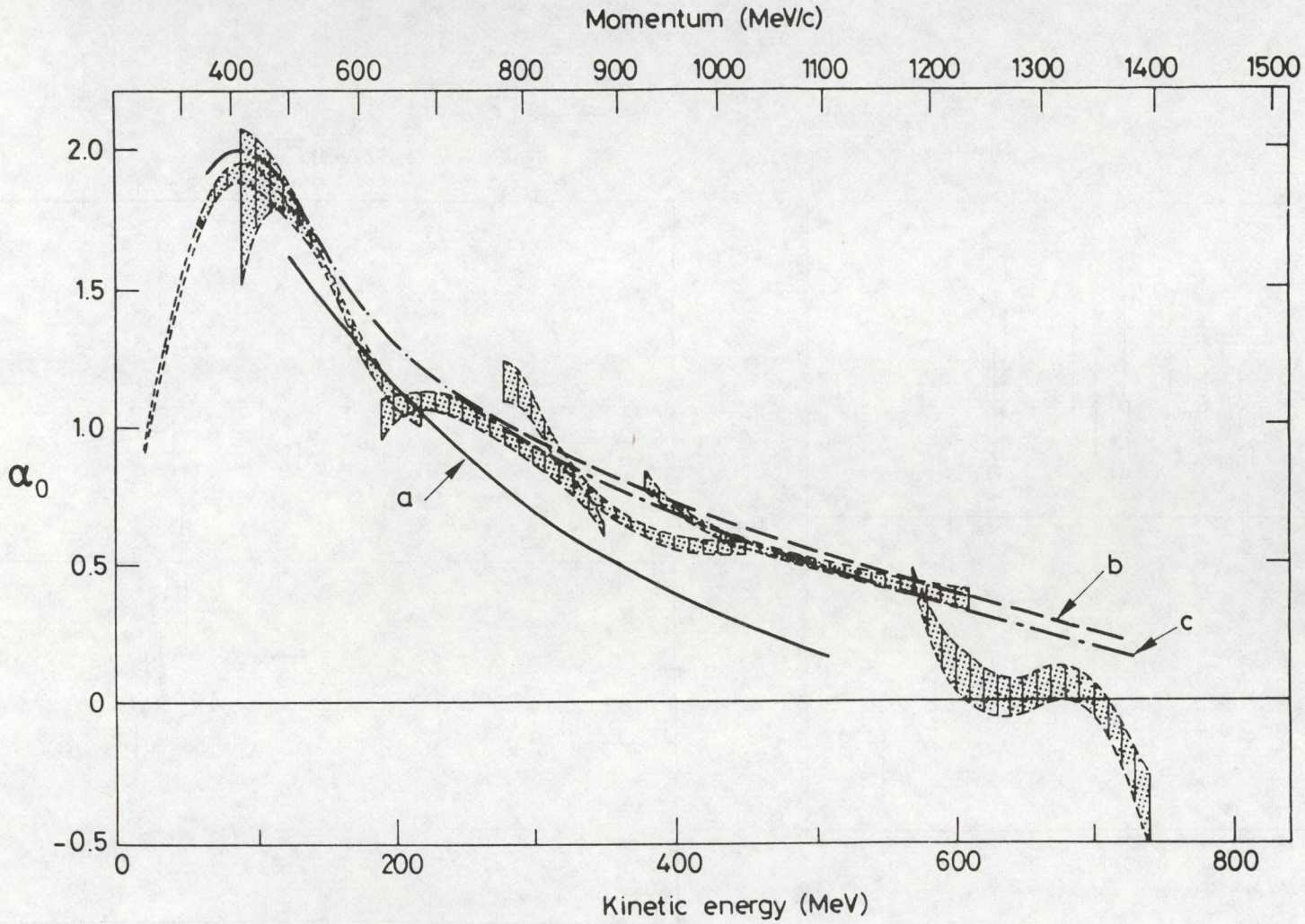
Momentum (MeV/c)
400
600
800
900
1000
1100
1200
1300
1400
1500
2.0
1.5
1.0
0.5
0
-0.5
α_0
a
b
c
0
200
400
600
800
Kinetic energy (MeV)

Fig. 6

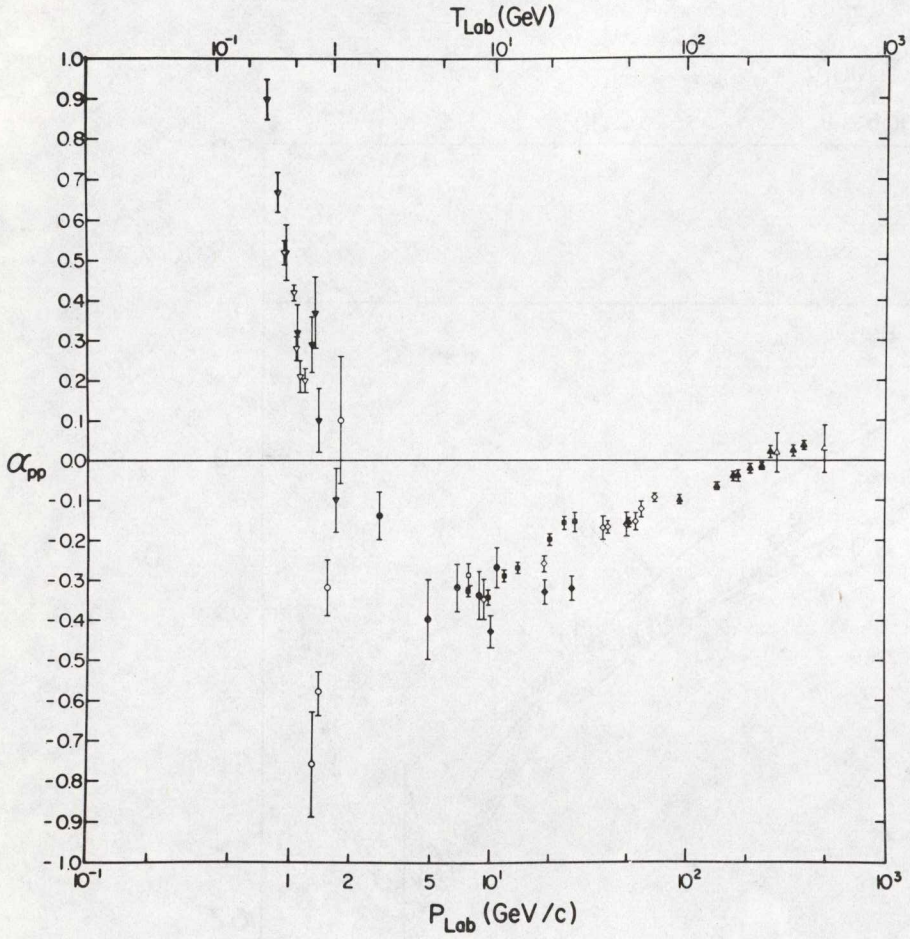

Fig. 7a

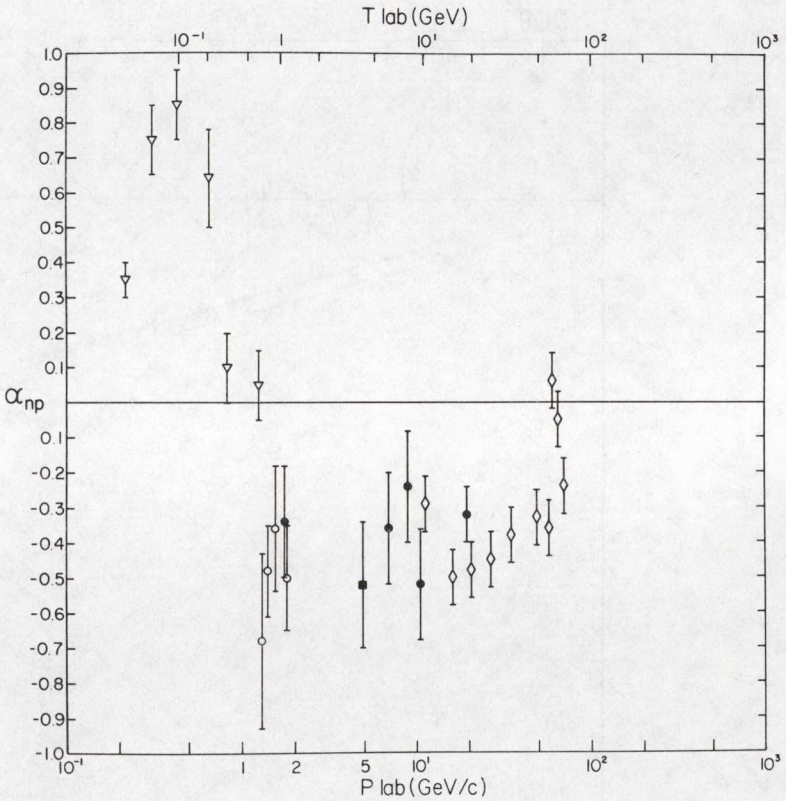

Fig. 7b

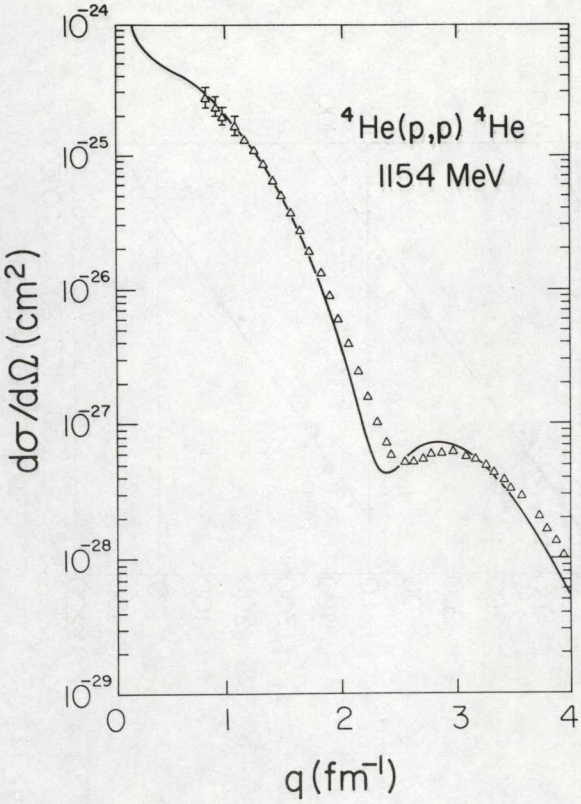

Fig. 8

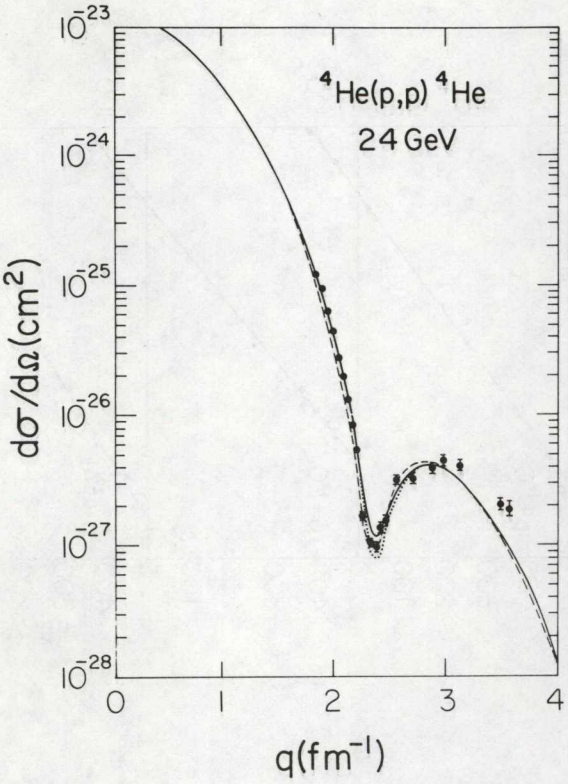

Fig. 9

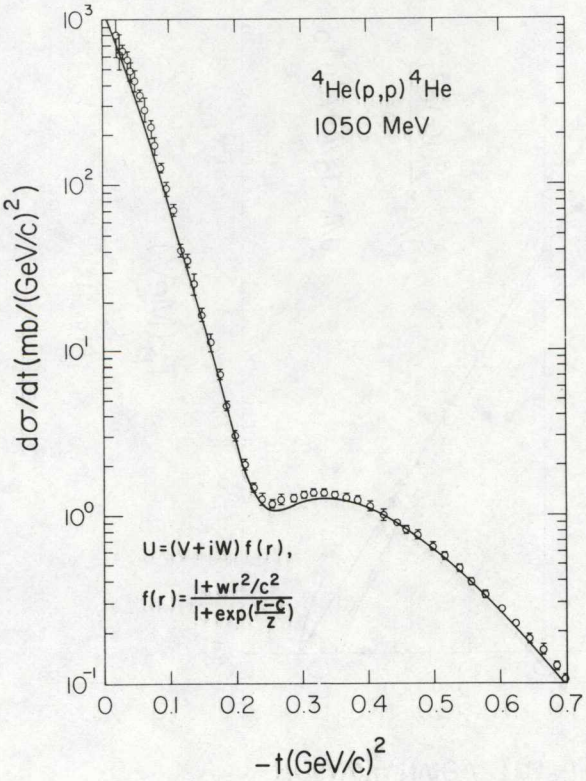

Fig. 10

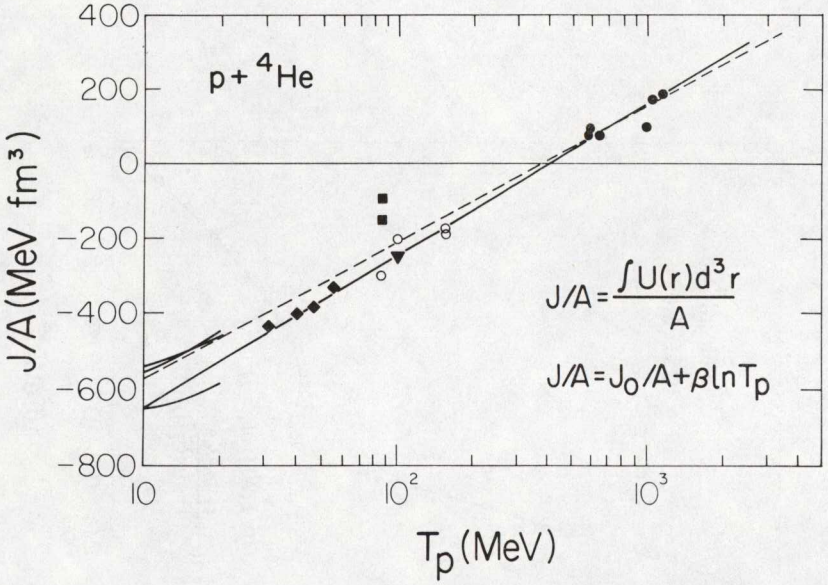
p + 4He
J/A (MeV fm3)
400
200
0
−200
−400
−600
−800
10
10^2
10^3
Tp (MeV)
J/A = ∫U(r)d3r / A
J/A = J0/A + β ln Tp

Fig. 11

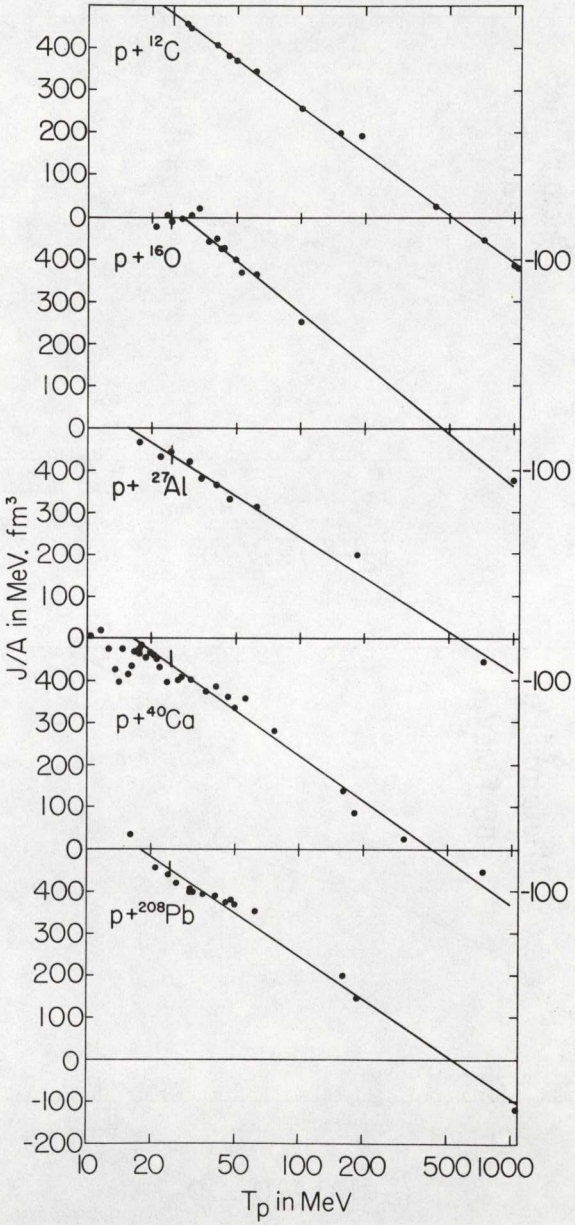
p + 12C
p + 16O
p + 27Al
p + 40Ca
p + 208Pb
J/A in MeV. fm3
400
300
200
100
0
-100
-200
10
20
50
100
200
500
1000
Tp in MeV

Fig. 12

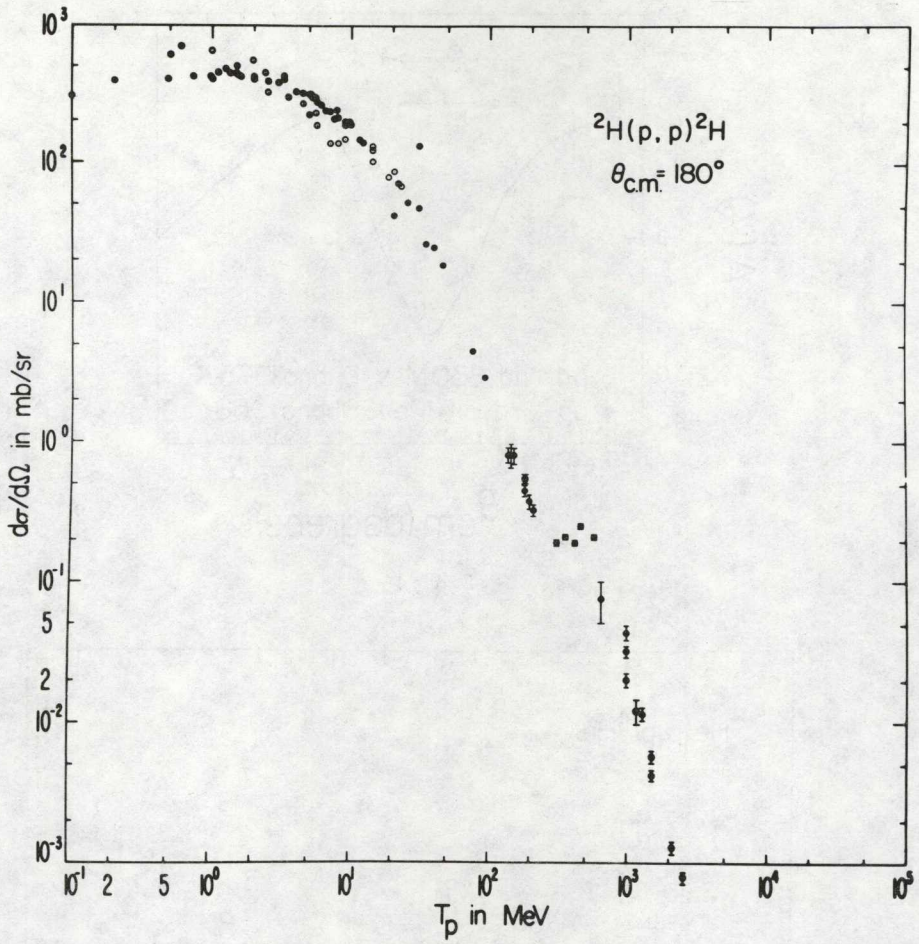
$^2H(p,p)^2H$
$\theta_{c.m.} = 180°$
$d\sigma/d\Omega$ in mb/sr
T_p in MeV

Fig. 13

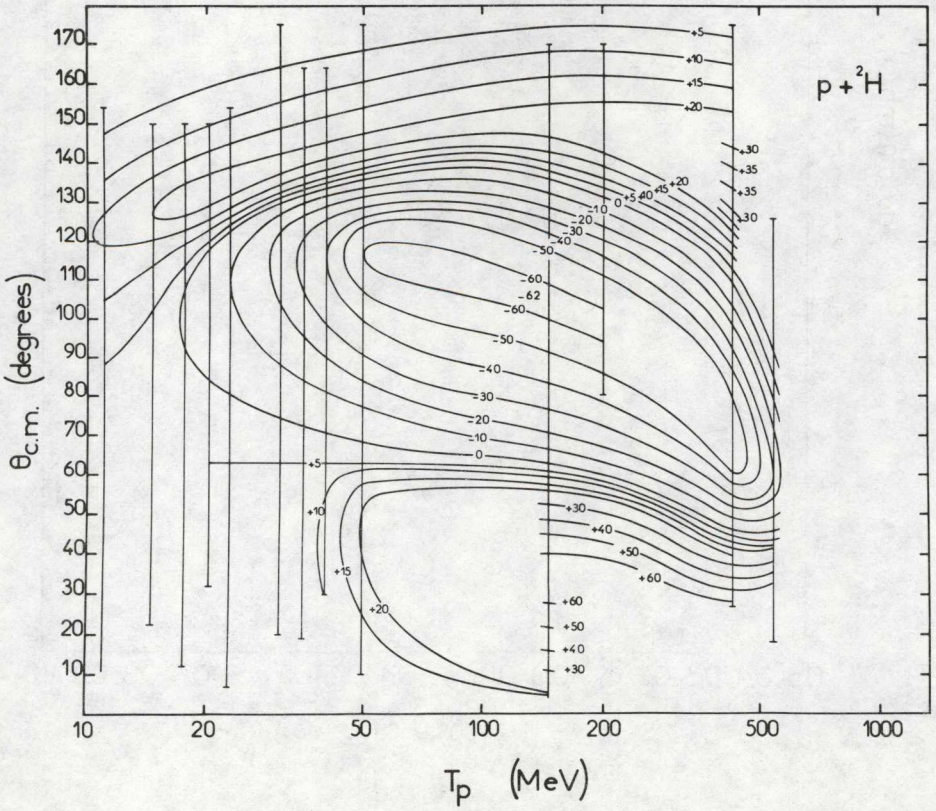
$p + {}^2H$
$\theta_{c.m.}$ (degrees)
T_p (MeV)

Fig. 14

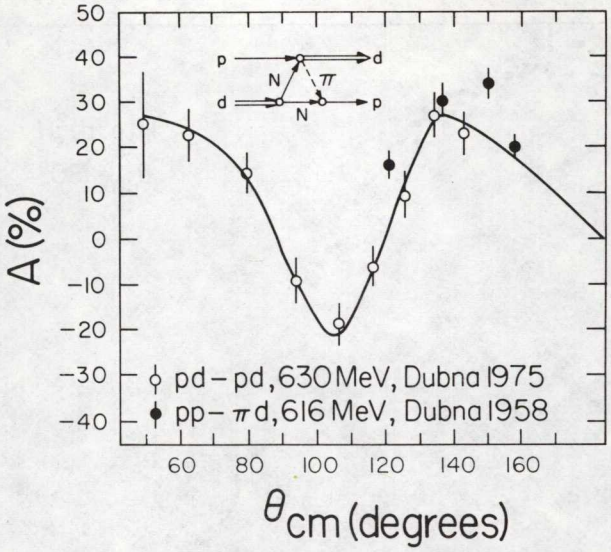
A (%)
θcm (degrees)
pd – pd, 630 MeV, Dubna 1975
pp – πd, 616 MeV, Dubna 1958
p
d
N
π

Fig. 15

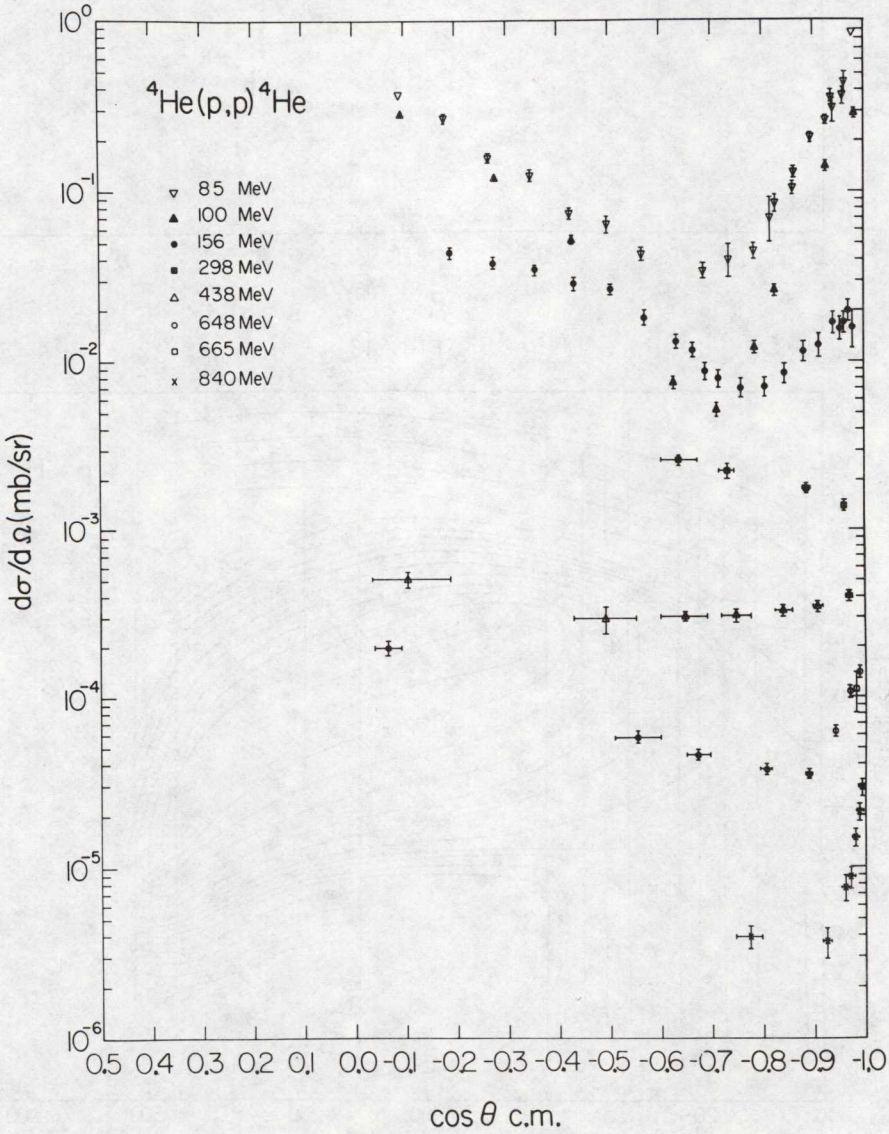
4He(p,p)4He
85 MeV
100 MeV
156 MeV
298 MeV
438 MeV
648 MeV
665 MeV
840 MeV
dσ/dΩ (mb/sr)
cos θ c.m.

Fig. 16

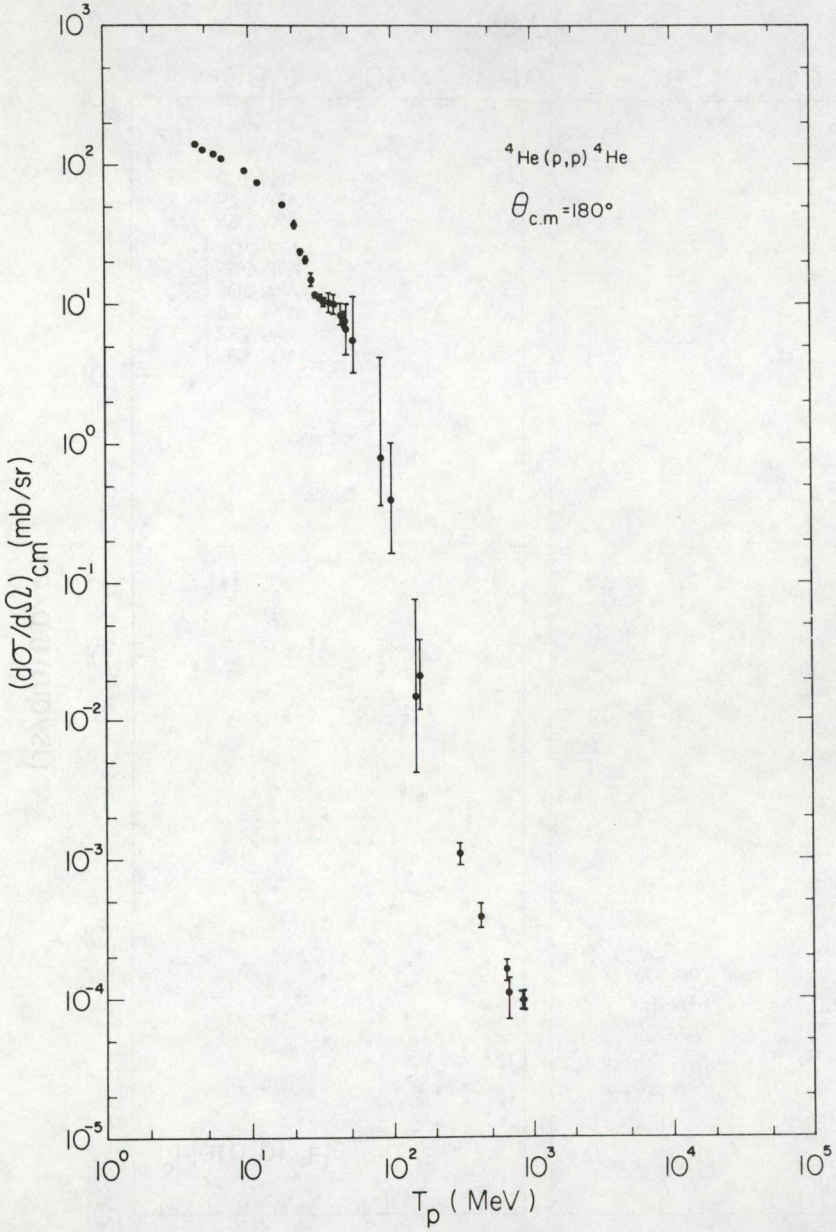
^{4}He (p,p) ^{4}He
$\theta_{c.m}$=180°
$(d\sigma/d\Omega)_{cm}$ (mb/sr)
T_p (MeV)

Fig. 17

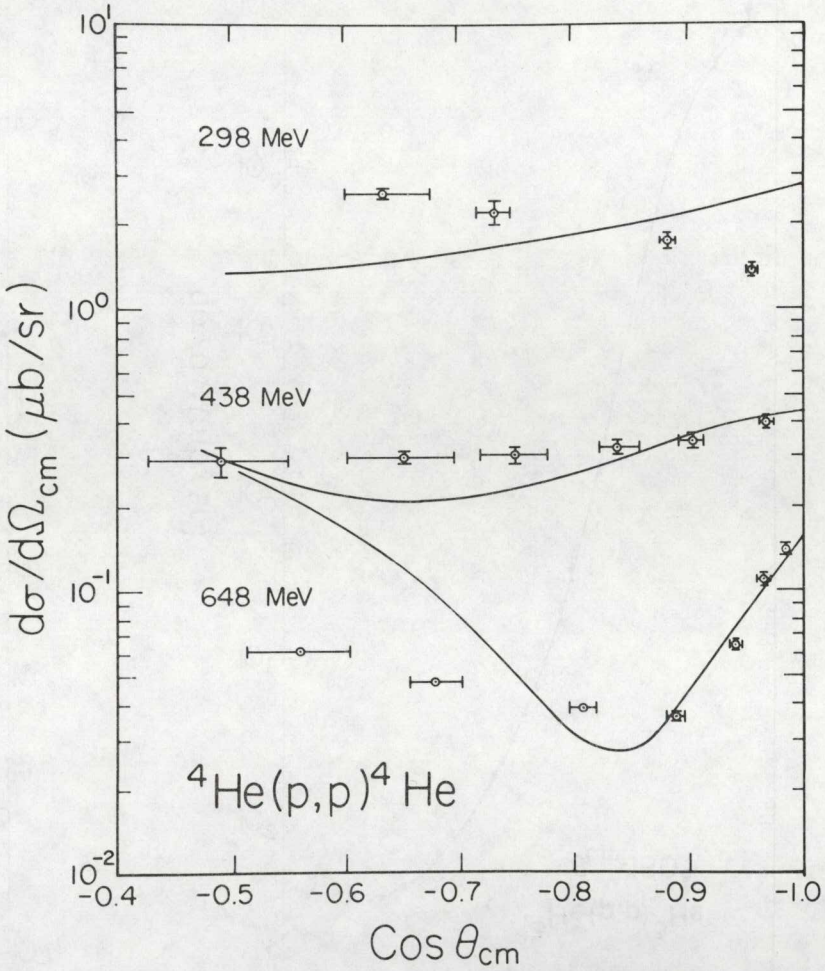
298 MeV
438 MeV
648 MeV
^{4}He(p,p)^{4}He
$d\sigma/d\Omega_{cm}$ (μb/sr)
Cos θ_{cm}

Fig. 18

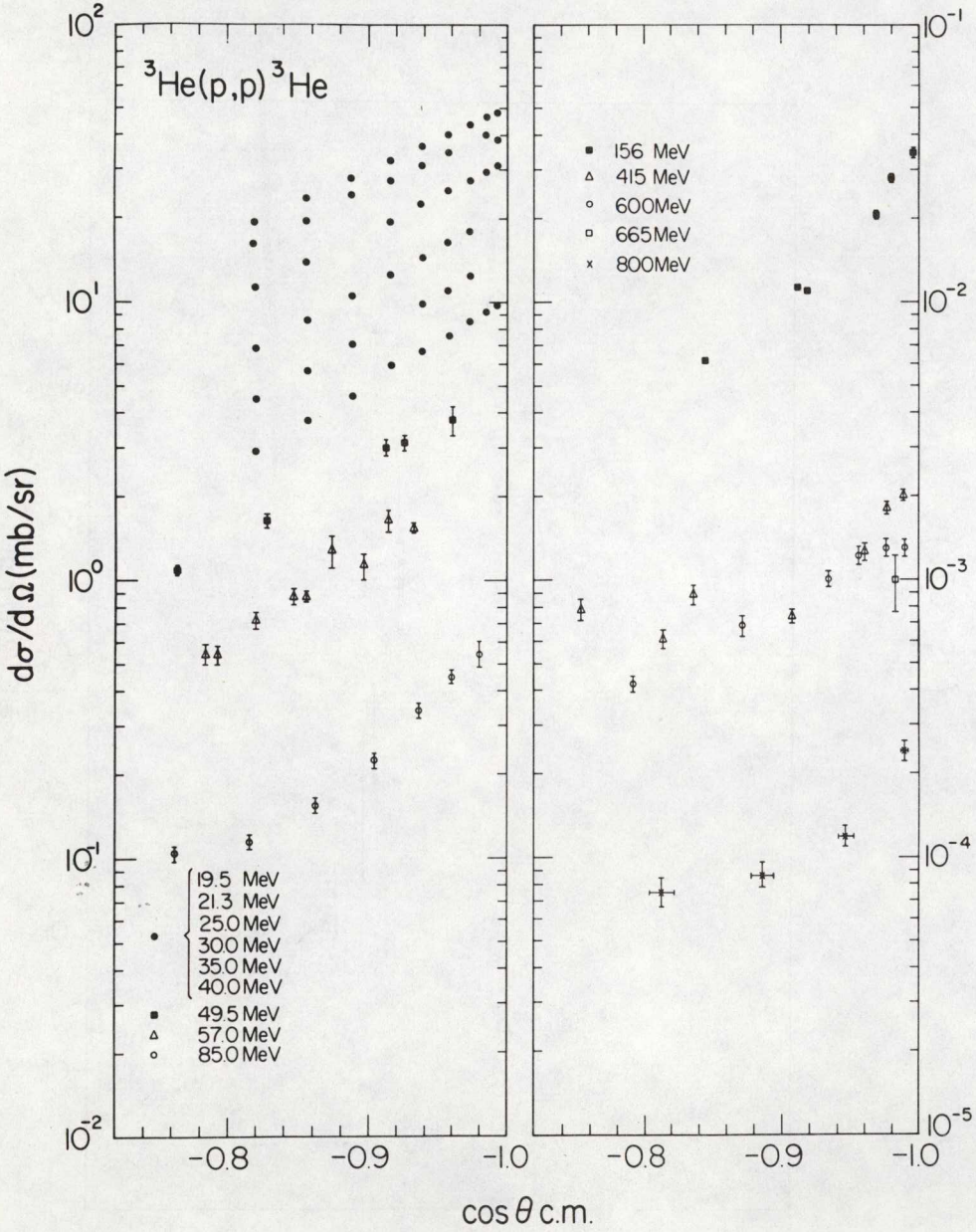
^{3}He(p,p)^{3}He
156 MeV
415 MeV
600MeV
665MeV
800MeV
19.5 MeV
21.3 MeV
25.0 MeV
30.0 MeV
35.0 MeV
40.0 MeV
49.5 MeV
57.0 MeV
85.0 MeV
dσ/dΩ (mb/sr)
cos θ c.m.

Fig. 19

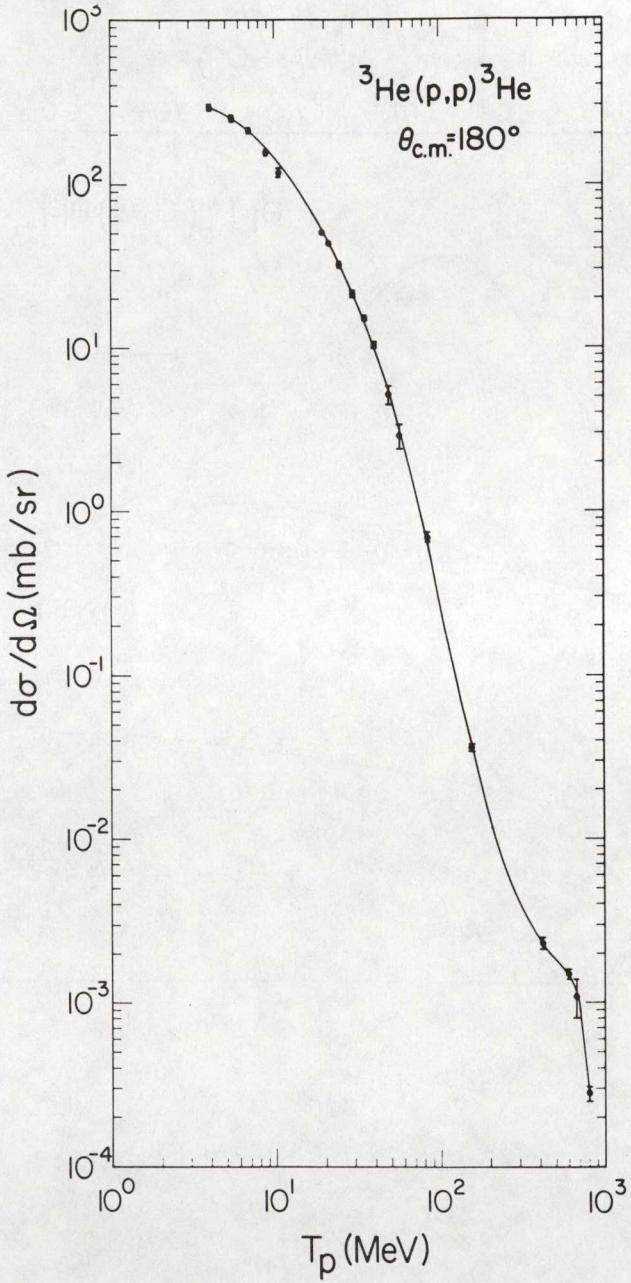
^{3}He(p,p)^{3}He
$\theta_{c.m.}$=180°
dσ/dΩ (mb/sr)
T_p (MeV)

Fig. 20